Frontiers in Heat and Mass Transfer (FHMT), 13, 16 (2019)
DOI: 10.5098/hmt.13.16

Global Digital Central
ISSN: 2151-8629

Frontiers in Heat and Mass Transfer

Available at www.ThermalFluidsCentral.org

WALL HEAT FLUX PARTITIONING ANALYSIS FOR SUBCOOLED FLOW BOILING OF WATER-ETHANOL MIXTURE IN CONVENTIONAL CHANNEL

B.G. Suhas [a, *], A. Sathyabhama [b], Kavadiki Veerabhadrappa [a], R. Suresh Kumar [a] and U. Kiran Kumar [a]

[a] *Mechanical Engineering Department, BMS College of Engineering, Bull temple road, Bengaluru-560019,India*
[b] *Mechanical Engineering Department, NITK, Surathkal, Mangalore-575025, India*

ABSTRACT

In the present study, heat transfer coefficient of water-ethanol mixture in the subcooled boiling region is determined in a rectangular conventional channel (Channel size ⩾3 mm). When the heat flux and mass flux increase it is observed that heat transfer coefficient increases. But the effect of heat flux is significant when compared with that of mass flux in the subcooled boiling region. It is found that maximum and minimum heat transfer coefficient are observed for mixture with 25% Ethanol volume fraction and 75% Ethanol volume fraction respectively. Wall heat flux partitioning analyses is carried out for mixture with different ethanol volume to determine the contribution of heat flux towards convection, agitation and evaporation. It is also found that heat flux due to convection decreases with increase in heat flux at partial and fully developed nucleate boiling heat regions for all volume fractions. The heat flux determined from the partitioning analysis are lower than the experimentally determined heat flux values at the partial nucleate boiling region and are higher at the fully developed boiling region.

Keywords: Agitation, Evaporation, Heat flux due to forced convection, Fully developed nucleate boiling, Partial nucleate boiling

1. INTRODUCTION

Subcooled boiling heat transfer characteristics in conventional channels are dominant parameters in the performance of cooling systems for heat dissipative devices like catalytic reactors, HEV batteries, electronic devices, radiators etc. used in nuclear, petroleum, chemical and automobile industries (Madhavi and Vivek. 2013). Subcooled boiling heat transfer characteristics in conventional channels for pure component have been extensively studied. In the past decades, refrigerants were mainly used as coolants. But the impact of these refrigerants on the environment in terms of global warming and ozone depletion has been identified in recent times (Weiwei and Fang, 2014). The use of binary mixtures is one of the better choice of a liquid that could be in competent to these coolants. The binary mixture like water-glycol is highly expensive and requires higher power to circulate due to high viscosity. Water-methanol, water-butanol and water-propanol are toxic in nature. For economical and environmental concern water-ethanol mixture is said to be best coolant to remove the heat from such heat dissipative devices.

Flow boiling of binary mixtures is found to be complex than the corresponding pure fluids due to the following reasons (a) boiling point temperature is not constant for mixture composition (b) The thermophysical properties of the binary mixture does not obey the linear mixing law (c) the transport mechanism is confined by the mass transfer process of the lower boiling component when phase changes, and (d) the bulk liquid contact angle, which is a primary concern to understand the boiling mechanism, follows non-linear behavior (Lixin and Dieter, 2006). The flow boiling has two regions, namely partial nucleate boiling and fully developed nucleate boiling. When the wall temperature is higher than the saturation temperature of the bulk liquid, nucleation of bubbles can be observed and is known as onset of nucleate boiling (ONB). At particular heat flux where bubbles lift off from the heated wall of the channel is called the location of onset of significant voids (OSV). The bulk liquid attains the saturation temperature and the bubbles begin to merge and coalesce with each other. This is called onset of saturated nucleate boiling (OSNB). The region between the ONB and OSV is called partial nucleate boiling. The region between OSV and OSNB is called subcooled nucleate boiling. The region of ONB and OSV can be identified by the wall heat flux partitioning analysis. The contribution of applied heat flux towards forced convection, agitation and evaporation in subcooled flow boiling region is analysed by heat flux partioning analysis (Vijay *et.al.*, 2007). The subcooled flow boiling of water-ethanol mixture is applicable to the operation of medium to small heat dissipative devices. It is well known that the operational temperature must be maintained to avoid any malfunction of these heat dissipative devices. Detailed investigation on subcooled flow boiling of water-ethanol mixture is scarce in literature which is essential to design the cooling devices. Considering this, the present study aims to determine the subcooled flow boiling heat transfer coefficients of water-ethanol mixture.

The models can be classified into types. One type is the empirical correlations heat transfer coefficient which are based on the experimental results. The other type includes semi-empirical correlations that includes partitioning of wall heat flux which is accountable for heat transfer through wall. Among these kinds of correlations, the mechanistic one of heat flux partitioning has been receiving many interests from recent studies on subcooled flow boiling (Chul *et al.*, 2017, Kim et al., 2018 and Hanyang Gu et al., 2019) The present work consist of determining the theoretical heat flux by wall heat flux partitioning analysis of water-ethanol mixtures for different heat flux, mass flux and inlet temperatures. The effect of heat flux due to forced convection, agitation and evaporation on the subcooled flow boiling heat transfer is determined. Effect on boiling heat transfer coefficient due to addition of ethanol to

*Corresponding author e-mail address: suhas_bg@yahoo.co.in

Global Digital Central
ISSN: 2151-8629

water in the subcooled boiling region at various volume fraction is also discussed.

2. METHODOLOGY

2.1 Experimental test set up and data reduction

The schematic diagram of the experimental test set up is shown in Fig. 1. The photographic images of the experimental set up are shown in Fig. 2 and 3.

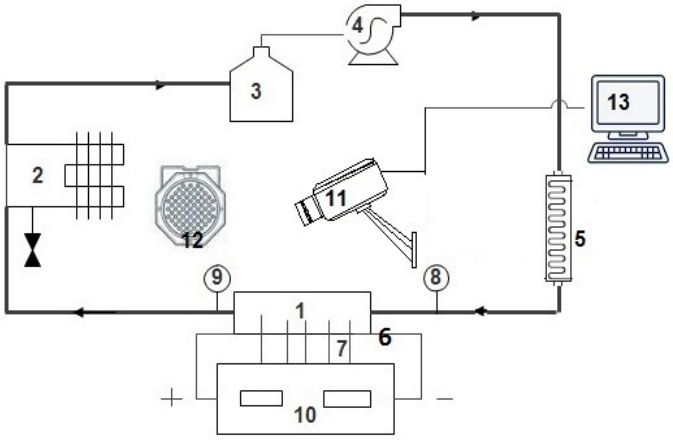

Fig. 1 Schematic diagram of experimental setup: (1) Rectangular aluminum block consisting of two rectangular channels, (2) Condenser coil dipped in ice water bath, (3) Reservoir (4) Peristaltic pump, (5) Preheater, (6) Cartridge heaters, (7) Thermocouples to measure wall temperature, (8) Thermocouple to measure fluid inlet temperature, (9) Thermocouple to measure fluid outlet temperature, (10) Temperature indicator panel, (11) High speed camera, (12) Light source, and (13) Data Aquisiation system for flow visualization

Fig. 2 Front view of the experimental setup: (1) High speed camera, (2) Condenser coil dipped in ice water bath, (3) Reservoir, (4) Peristaltic pump, (5) Preheater, (6) Temperature indicator panel, and (7) Light source

The experimental set up consist of a closed loop comprising of a subcooler, reservoir, preheater and pump with variable flow rate. Two channels of 0.01 m (width) × 0.01 m (height) × 0.15 m (Length) is considered in an aluminum blocks. Two cylindrical cartridge heaters are placed inside the aluminum block at the distance of 40 mm below the channels. The thermocouples are sued to measure wall temperatures, the inlet and outlet temperatures of the fluid flowing through the channel. The temperature readings are displayed on the temperature indicator panel. Heat flux is determined by temperature gradient that exist between the first row and second row of thermocouples that are arranged in aluminum block. The first row of five thermocouples are placed 2 mm below the channel in a row. The second row of five thermocouples are placed 20 mm below the first row of thermocouple as seen in Fig. 4. Heat loss is prevented by providing mineral wool as insulating material. Specifications of the equipments used are shown in Table 1 and Table 2 (Suhas and Sathyabhama, 2017; Suhas and Sathyabhama, 2018; Suhas and Sathyabhama, 2018).

Fig. 3 Rear view of the experimental setup: (1) Rectangular aluminum block consisting of two rectangular channels, (2) Thermocouples to measure wall temperature, (3) Thermocouple to measure channel inlet temperature , and (4) Thermocouple to measure outlet fluid temperature

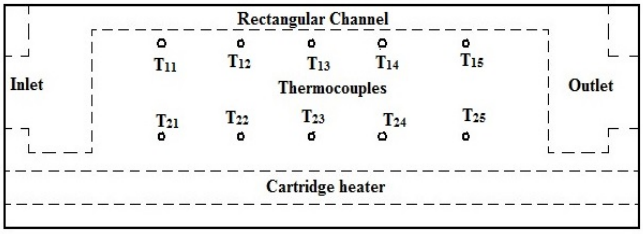

Fig. 4 Arrangement of thermocouples in the cold plate.

Table 1 Instruments and equipment used in the present experiment

Instrument/Equipment	Specifications
k-type thermocouple (12 no's)	Range :-20℃ to 400℃ Sheath length: 20 mm Sheath diameter: 1.2 mm
Cartridge heater (2 no's)	Diameter: 12.7 mm Length: 150 mm Capacity: 750 W
Peristaltic pump	Capacity: 100 liters per hour Operating pressure: Atmospheric
Preheater	Chamber capacity: 4 Liters Heater capacity: 3 kW

Table 2 Specifications of high speed camera and source light

Processor	AOS Promon 501
Lens	50 mm
Aperture setting	f/1.4 D
Shutter speed	1/15
Frames per second	1459
Resolution	480×240 pixels
LED PAR Light	Slim die cast body, Power 120W, beam 25 degree, CRI>85, DMX 512 Auto, sound active, 3 section lightweight aluminum stand

2.2 Uncertainty

International Bureau of weights and measures (IBWM) and International organization of standards (ISO) random defines the independent variables by using root-sum-square (RSS) of standard deviation as shown in Equation (1).

$$\omega_{ip} = \sqrt{\omega_{iresolution}^2 + \omega_{iconversion}^2 + \omega_{icalibration}^2 + s_{2\sigma_i}^2} \quad (1)$$

The uncertainties of calculated parameters can be determined after finding the uncertainty of independent variables (Kline and McClintock, 1953), by using Equation (2).

$$\omega_{cp}^2 = \sum_{i=1}^{n} \left(\frac{\partial f}{\partial x_i}\right)^2 \omega_{x_i}^2 \quad (2)$$

Table 3 shows the corrected values applied to obtain actual values of temperature..

Table 3 Constants for temperature measurement corrections

Readings	Steam point (K)	Ice point (K)	a	b
T1	372.3	274.1	1.02	-6.58
T2	375.4	275.2	1	-2
T3	374.3	275.1	1.01	-4.77
T4	375.1	275.3	1	-2
T5	374.3	273.1	0.99	2.71
T6	374.2	273.2	0.99	2.71
T7	373.3	274.2	1.01	-3.76
T8	375.2	274.1	0.99	1.71
T9	373.2	275.2	1.02	-7.61
T10	373.1	274.3	1.01	-3.76
T11	372.1	273.2	1.01	-2.75
T12	371.4	275.1	1.04	-1.45

Uncertainties in measured and calculated parameters are shown in Table 4. It is observed that the all measured temperature readings fluctuated within ± 0.3 ºC after the stabilized period of two hours.

Table 4 Uncertainties of measured and calculated parameters

Parameter	Uncertainty
Temperature (K)	± 0.35℃ (RSS)/ ± 0.1℃
Mass flow rate (kg/s)	$\pm 2.32\%$
Mass flux (kg/m^2-s)	$\pm 0.77\%$
Heat flux (kW/m^2)	$\pm 13.3\%$
Heat transfer coefficient (kW/m^2-K)	$\pm 9.11\%$

The voltage resolution is at a 100 mv and the range signal is 0.01mv. The standard deviation is found to be $\pm \mathbf{0.15°C}$. The combined uncertainty of the temperature measurements is calculated by Equation (2).

3. RESULTS AND DISCUSSIONS

The experiment is conducted to determine the heat transfer coefficients of water-ethanol mixture (0%, 25%, 50%, 75% and 100%) in the subcooled flow boiling region for various parameters such as heat flux mass flux, channel inlet temperature. Table 5 shows the operating conditions that are carried out during experimentation.

Table 5 Operating conditions in the present experiment

Parameter	Operating Range				
	Pure water	25% Ethanol volume fraction	50% Ethanol volume fraction	75% Ethanol volume fraction	Pure ethanol
Hydraulic Diameter (mm)	10				
Heat flux (kW/m^2)	21.78 35.11 45.33 62.33 78.4 90.4 100.5 109.6 121.9 133.4	21.78 35.11 45.33 62.33 78.4 90.4 100.5 109.6 121.9	21.38 35.11 45.33 62.33 78.4 90.4 100.3 109.6	21.78 35.11 45.33 62.33 78.4 90.4 100.3	21.78 35.11 45.33 62.33 78.4 90.4
Mass flux (kg/m^2-s)	76.67, 91.33, 115.33,151.67, 228.33				
Channel inlet temperature (K)	303, 313, 323				

3.1 Validation

The experimental values obtained for water are validated with available literature correlations. The Mean absolute error (MAE) of Nusselt number for water which are determined experimentally and those predicted from the correlations is calculated by Equation (3).

$$MAE = \frac{1}{n}\sum \left|\frac{Predicted\ values - Experimental\ values}{Predicted\ values}\right| \times 100 \quad (3)$$

The comparison of heat transfer coefficient data of water with those predicted using available literature correlations are seen in Fig. 5. Gungour and Winterton correlation (1986), Kandlikar correlation (1998), Liu-Winterton correlations (1991) and Chen correlation (1966) predicted the experimental values with mean absolute error (MAE) of 8.82%, 11.46%, 13.31% and 21.37% respectively. It can be seen that the Chen correlation under predicted the experimental results. These deviation are mainly due to:

i) Non uniform temperature distribution in cold plate

ii) The assumption of one dimensional temperature distribution to calculate heat flux.

The Gungour –Winterton and Kandlikar correlations predicted the experimental values better when compared with that of Chen and Liu-Winterton correlations because of Boiling number in Gungour-Winterton and Kandlikar correlations.The boiling number plays a major role in subcooled flow boiling region. It is also proved to be significant while predicting the subcooled flow boiling heat transfer coefficient by heat transfer approach (Claudi, 2010). When there is an increase in heat flux,

Global Digital Central
ISSN: 2151-8629

the nucleation sites are activated in large numbers. After bubble nucleation, the layer of superheated liquid mixes well with the subcooled liquid at the top layer leading to agitation (Minxia *et al*., 2013). The heat flux can be considered as the net effect of transient heat transfer around the nucleation sites and micro-layer evaporation beneath the bubbles. The departed bubble removes the heat from the channel wall.

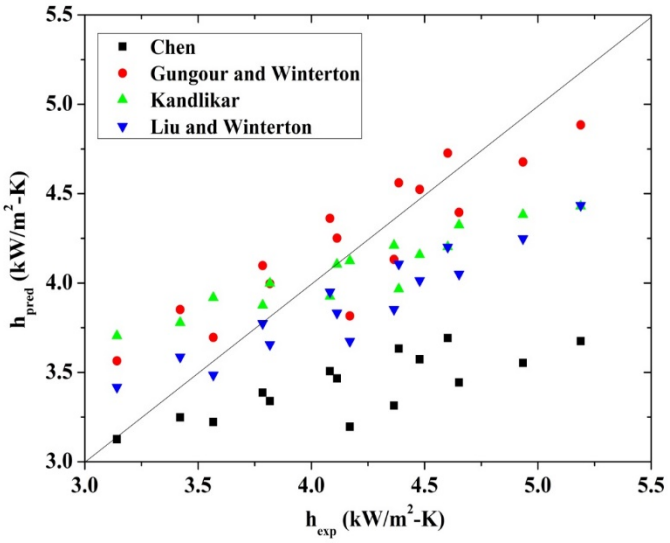

Fig. 5 Comparision of subcooled flow boiling heat transfer coeffcient values of water with correlations.

3.2 Results on subcooled flow boiling

The variation of subcooled flow boiling heat transfer coefficient with ethanol volume fraction at various inlet temperatures at heat flux of 90.4 kW/m^2 is shown in Fig. 6.

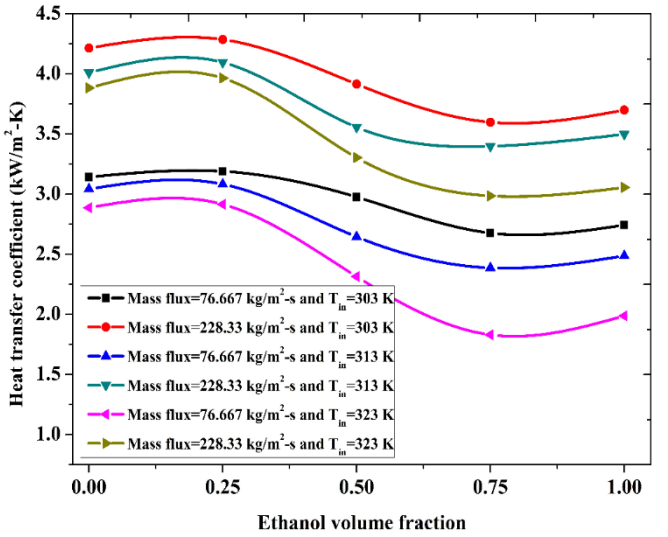

Fig. 6: Variation of subcooled flow boiling heat transfer coefficient with ethnaol volume fraction

The subcooled boiling takes place for both water and ethanol at this particular value. If the heat flux is lesser than 90.4 kW/m^2, heat transferred to water will lead forced convection and not subcooled boiling. If the heat flux is greater than 90.4 kW/m^2, saturated boiling of ethanol will commence. It is seen that the heat transfer coefficient increases for mixture with the 25% ethanol volume fraction. But with further addition of ethanol, the heat transfer coefficient reduces. For 25% volume fraction, difference between dew point temperature (T_d) and bubble point temperature (T_b) is obtained to be maximum and thus indicates the widest region of coexisting liquid vapour (Suhas and Sathyabhama, 2017; Fu *et al*., 2013). The wide range of coexisting region is observed due to an increase in evaporative heat flux for mixture with 25% ethanol volume fraction as shown in Fig. 7. For mixture with 25% ethanol volume fraction, the higher volatile component near the wall of the channel induces temperature gradients in the micro layer region. This gradient causes the Marangoni force to push the bulk liquid towards the liquid vapour interface which causes agitation and thus increases the heat transfer.

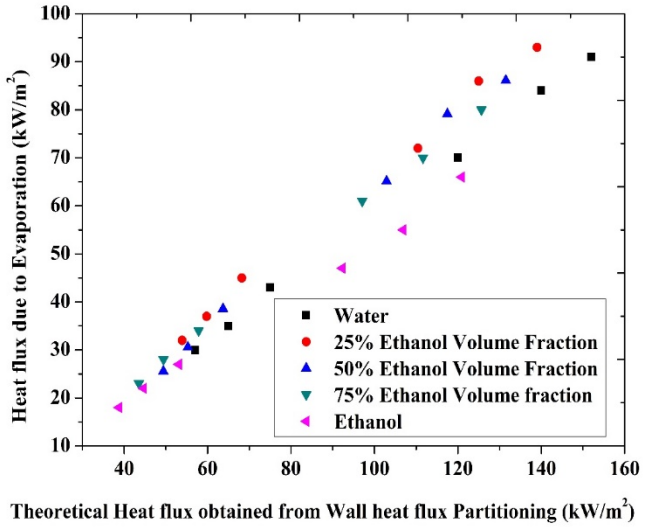

Fig. 7 Variation of heat flux due to evaporation with theoretical heat flux obtained due to wall heat flux partitioning

3.3 Wall heat flux Partitioning

In the present work the region of ONB and OSV are determined by Unal (1975) correlation as given by Equation (4) and (5). This correlation was chosen because it is difficult to determine the experimental values of heat flux required for ONB and OSV.

$$\frac{h\Delta T_W}{q''} = 0.24 \text{ when } u \geq 0.45\ m/s \quad (4)$$

$$\frac{h\Delta T_W}{q''} = 0.11 \text{ when } u < 0.45\ m/s \quad (5)$$

Equation (5) is preferred because the velocity is found to be less than 0.45 m/s in the present experiment. When $\frac{h\Delta T_W}{q''}$ exceeds 0.11, heat flux value chosen is found to be in the fully developed nucleate boiling region. When $\frac{h\Delta T_W}{q''}$ is less than 0.11, the heat flux is found to be in the partial nucleate boiling region.

3.3.1 Partial nucleate boiling

Bowring (1962) suggested superposition method to determine the heat flux in partial nucleate boiling as given by Equation (6) and Equation (7). The heat flux supplied is partioned as heat flux due to forced convection and heat flux due to evaporation of the micro layer of the liquid above the wall surface.

$$q_{pnb} = q_{fc} + q_{ev} \quad (6)$$

$$q_{fc} = \frac{kNu}{d_{hyd}}(T_{sat} - T_l) \quad (7)$$

Single phase forced convective heat transfer coefficient can be calculated by Dietus Botler Equation (8).

$$Nu = 0.023 Re^{0.8} Pr^{0.4} \quad (8)$$

The evaporative heat flux is considered as fully developed nucleate pool boiling by Bergles and Roshsenow (1964) as given by Equation (9). The evaporation above the heated wall is due to the phase change of liquid if it would be in pool boiling condition (Vijay and Gopinath, 2006).

$$q_{ev} = q_{nb} = \mu_l h_{fg} \sqrt{\frac{g(\rho_l - \rho_v)}{\sigma_s}} Pr^{m/n} \left(\frac{c_{p,l}[T_{wall} - T_{Sat}]}{C_s h_{fg}}\right)^{1/n} \quad (9)$$

Global Digital Central
ISSN: 2151-8629

q_{ONB} and ΔT_{wONB} can be predicted by Equation (10) and (11) as given below:

$$q_{ONB} = q_{nb}\left\{1 - \left[\left(\frac{q_{nb}}{q_{fc}}\right)^2 - 1\right]\left(\frac{q_{fc}}{q_{nb}}\right)\right\} \quad (10)$$

$$\Delta T_{wONB} = \left(\frac{q_{ONB}}{5.3p^{1.156}1.8^{2.41/p^{0.0234}}}\right)^{p^{0.0234}/2.41} \quad (11)$$

Bjorge (1982) suggested using Equation (12) to predict the wall super heat during partial nucleate boiling.

$$\Delta T_{wpnb} = \frac{\Delta T_{wONB}}{\left(1-\sqrt{\frac{q_{pb}^2-q_{fc}^2}{q_{nb}^2}}\right)^{1/3}} \quad (12)$$

3.3.2 Fully developed nucleate boiling (Subcooled nucleate boiling)

Bowring (1962) developed superposition method to determine the heat flux in fully developed nucleate boiling region as given by Equation (13).

$$q_{fdb} = q_{fc} + q_{ev} + q_a \quad (13)$$

Agitation heat flux (q_a) results from the thermal boundary layer during bubble growth and lift-off and is given by Equation (14). This is due to replacing the adjacent cold liquid in the departed site.

$$q_a = N_a f V_b C_{pl} \Delta T_w \quad (14)$$

Nucleation site density (N_a) is calculated by Equation (15) and (16).

$$N_a = 0.34 \times 10^4 (1 - cos\theta)\Delta T_W^2 \qquad \Delta T_{ONB} < \Delta T_w < 15K \quad (15)$$

$$N_a = 0.34 \times 10^4 (1 - cos\theta)\Delta T_W^{5.3} \qquad 15K < \Delta T_w \quad (16)$$

Bubble frequency (*f*) is calculated by Equation (17)

$$f = \frac{1}{t_w + t_g} \quad (17)$$

Where t_w is called bubble waiting period and t_g is called bubble growth period.

Wall superheat in fully developed nucleate boiling (OSV region) can be estimated by Engelberg-Foster and Grief correlation as given by Equation (18).

$$\Delta T_{wOSV} = \frac{0.7 q_{fdb}}{h_{fc}} - 7.8exp[-0.0163(p-1)]\left(0.7 q_{fdb}\right)^{0.25} \quad (18)$$

Where, ΔT_{wOSV} is wall super heat at onset of vapour generation.

Sekoguchi et al (1980) developed an empirical correlation for the wall super heat at commencement of fully developed boiling region as given by Equation (19).

$$\Delta T_{wOSV} = 13.5 \frac{h_{fg}}{C_{p,l}}\left(\frac{q*_{avg}}{h_{fg}G}\right)^{0.65} \quad (19)$$

Where, $q*_{avg}$ is considered as the average of predicted values of heat flux. The average is calculated by the heat flux value that is considered in the partial nucleate boiling region and the first value of the heat flux which falls under fully developed nucleate boiling region.

Ahmad (1970) developed an empirical correlation assuming the wall temperature at OSV to be equal to the saturation temperature which is represented by Equation (20)

$$\frac{h_{OSV} d_h}{k_l} = 2.44\left(\frac{\rho_l d_h v_l}{\mu_l}\right)^{0.5}\left(\frac{C_{p,l}\mu_l}{k_l}\right)^{0.333}\left(\frac{h_{in}}{h_{fg}}\right)^{0.333}\left(\frac{h_{fg}}{h_l}\right)^{0.333} \quad (20)$$

Unal correlation (1975) is used to predict the heat flux when the OSV occurs which is given by Equation (21).

$$q_{OSV} = \frac{h_{OSV}\Delta T_{w,OSV}}{0.11} \quad (21)$$

Mixture properties of water-ethanol like thermal conductivity, liquid viscosity and surface tension are calculated by Flippov (1968), McLaughlin Equation (Deam and Mattox, 1970) and Macleoad-Sudgen correlation (Moles and Shaw, 1972) represented in the Equation (22), Equation (23) and Equation (24) respectively

$$\frac{k_m - k_i}{k_j - k_i} = C m_{fj}^2 - m_{fi}(1 - C) \quad (22)$$

$$ln(\mu_m) = x_i ln\mu_i + x_j ln\mu_j \quad (23)$$

$$\sigma_m^{1/4} = Pa_j(\rho_{Lm}x_j - \rho_{lv}y_j) \quad (24)$$

The value of mixture constant C in Equation (22) can be chosen as 0.72 (Mcniel et al., 2010).

3.3.3 Estimation of heat flux due to forced convection, evaporation and agitation

The variation of heat flux with wall super heat for water-ethanol mixtures at different ethanol volume fractions, at constant mass flux of 115.33 kg/m^2-s and inlet temperature of 303 K are shown in Fig. 8 to 12. It is observed that there is significant increase in heat flux at the subcooled flow boiling region when compared with that of forced convective region. Theoretical heat flux are lower than the experimentally determined heat flux values in the partial nucleate boiling region, but the theoretical heat fluxes are higher than the experimentally determined heat flux values in fully developed nucleate boiling region. It can also be seen that the region of ONB and OSV decreases with decrease in heat flux when the mixture with ethanol volume fraction increases. This is because the components in the liquid mixture have different boiling points. The lower boiling component breaks away from the liquid-vapor interface and the higher boiling component gets accumulated near layer of the concentration gradient near this interface (Minxia *et al*., 2012). Fig.13 show the variation of heat flux due to convection, evaporation and agitation with experimentally determined heat flux and the contribution to heat transfer by wall heat flux for pure water. Similar results are obtained for different ethanol volume fraction.

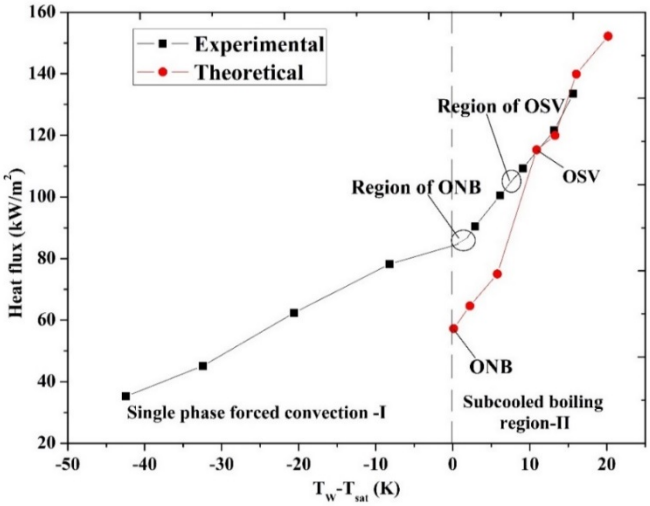

Fig. 8 Variation of heat flux with wall superheat for water.

Fig. 14 shows the percentage contribution to heat transfer among three heat fluxes, i.e heat flux due forced convection, evaporation and agitation. It can be observed that the heat flux due to forced convection decreases with increase in experimentally determined heat flux in partial nucleate and fully developed nucleate boiling regions. This implies that the increase in mass flux is not significant in these regions. Hence agitation due to bubble and heat transfer decreases with increase in inlet temperature. Heat flux due to evaporation and agitation increases with increase in heat flux. Fully developed nucleate boiling occurs when heat flux value exceeds 100 kW/m^2. Above this value of heat flux, agitation occurs.

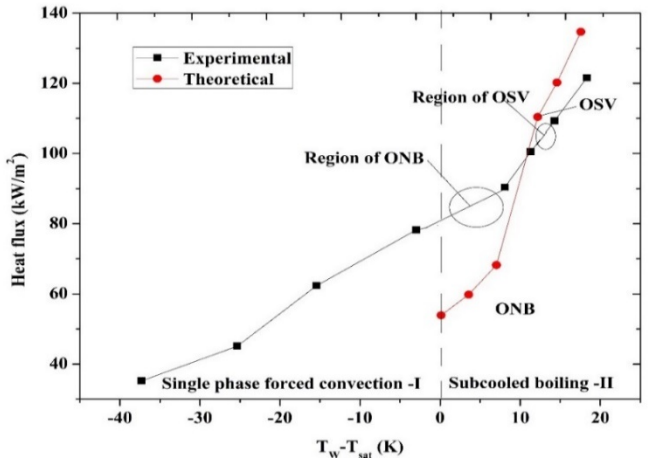

Fig. 9 Variation of heat flux with wall superheat for water-ethanol mixture of ethanol volume fraction of 25%.

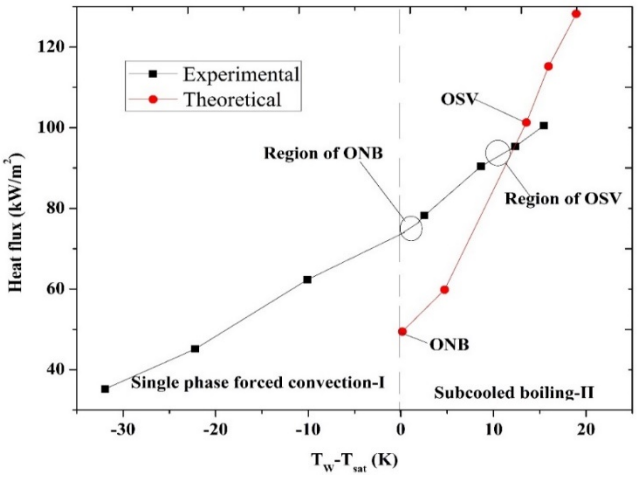

Fig. 10 Variation of heat flux with wall superheat for water-ethanol mixture of ethanol volume fraction 50%.

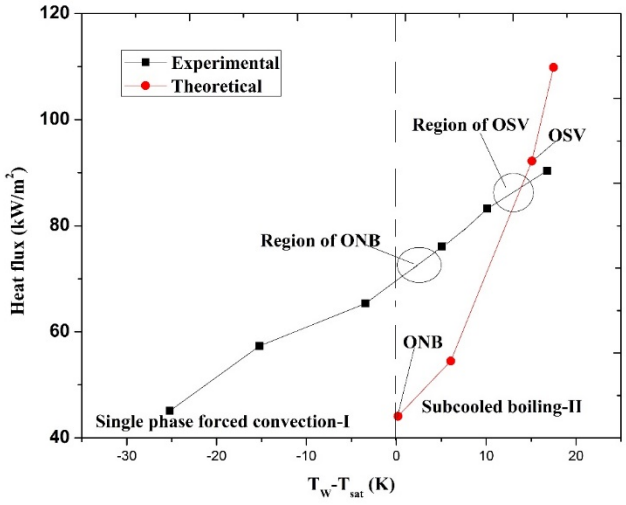

Fig. 11 Variation of heat flux with wall superheat for water-ethanol mixture of ethanol volume fraction 75%

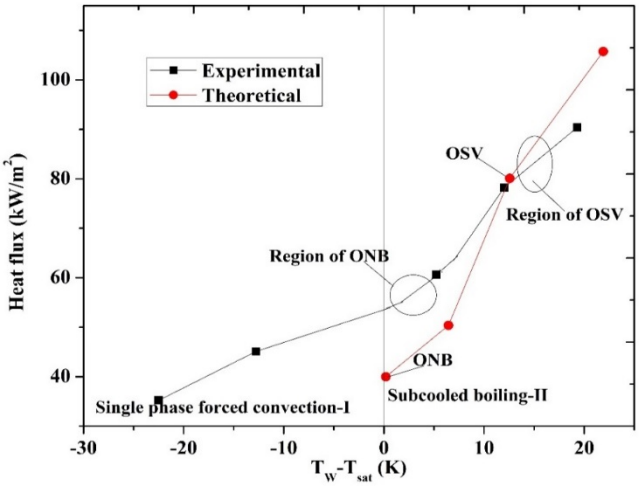

Fig. 12 Variation of heat flux with wall superheat for ethanol

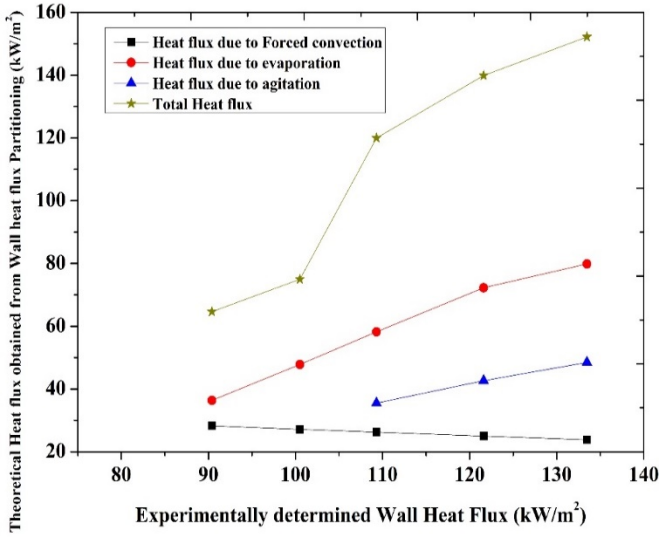

Fig. 13 Variation of theoretical heat flux with experimentally determined heat flux for water

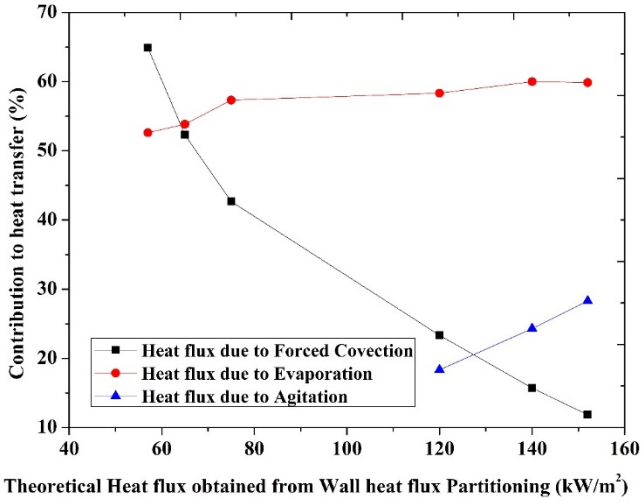

Fig. 14: Percentage contribution of heat flux to heat transfer in wall heat flux partitioning analyses for pure water

Global Digital Central
ISSN: 2151-8629

4. CONCLUSIONS

The heat transfer coefficient of water-ethanol mixture in the subcooled flow boiling region is determined for various parameters such as heat flux, mass flux and inlet temperature. The wall heat flux partioning analysis is carried out to determine the regions of Onset of Nucleate boiling and Onset of Vapour generation and the following conclusions can be arrived:

- It is seen that increase in heat flux and mass flux increases heat transfer coefficient in the subcooled flow boiling regions.
- However, the increase in heat flux proved to be significant to increase in heat transfer coefficient in the subcooled flow boiling region when compared with that of mass flux.
- It is observed that the high values of heat transfer coefficient is obtained with the addition of ethanol to water inititially upto 25% ethanol volume fraction.
- But at 50% and 75% ethanol volume fractions the heat transfer coefficient reduces.
- The pure ethanol has marginally higher value of heat transfer coefficient than the mixture of 75% ethanol volume fraction.
- From the wall heat flux partition analysis, it is found that only the heat flux due to forced convection decreases at partial and fully developed nucleate boiling regions for all values of ethanol volume fractions.

ACKNOWLEDGEMENTS

Authors wholeheartedly thank the management of NITK and BMS College of Engineering for extending their support for this work.

NOMENCLATURE

Bo	Boiling number
C_p	Specific heat (kJ kg^{-1}-K^{-1})
C	Mixture Constant
d	Diameter (m)
d_h	Hydraulic diameter (m)
F_x	Force parallel to flow direction (N)
f	Bubble frequency (s^{-1})
h	Heat transfer coefficient (kWm^{-2}-K^{-1})
h_{fg}	Latent heat of vaporization (kJkg^{-1})
k	Thermal conductivity (Wm^{-1}-K^{-1})
m	Mass flow rate
N_a	Nucleation site density (m^{-2})
Nu	Nusselt number
n	Number of readings
Pr	Prandtl number
p	Pressure (bar)
Re	Reynolds number
q	Heat flux (kWm^{-2})
t	Time (ms)
T	Temperature (K)
σ_i	Standard deviation

Greek Symbols

Δp_{Sat}	Difference between the saturated pressure and vapour pressure (bar)
ΔT	Temperature difference (K)
ΔT_W	Wall superheat (K)
ρ	Density (kgm^{-3})
μ	Dynamic viscosity (kgm^{-1}-s^{-1})
ω	Uncertainty

Subscript

a	Agitation
cr	Critical
d	Dew point
dep	Departure
ch	Channel
cp	Calculated parameter
Exp	Experimental
ev	Evaporation
f	Fluid
fc	Forced convection
fdb	Fully developed Boiling
fr	First row
fw	Wall and fluid
hyd	Hydraulic
i	First sample
i+1	Next sample
in	Inlet
ip	Independent parameter
ONB	Onset of Nucleate Boiling
OSV	Onset of Vapour Generation
nb	Nucleate Boiling
pb	Pool Boiling
l	Liquid
Sat	Saturated
Sr	Second row
s	Single phase
tp	Two phase
w	Waiting
W	Wall

REFERENCES

Ahmad, S. Y., 1970, "Axial distribution of bulk temperature and void fraction in a heater channel with inlet subcooling," *Journal of Heat Transfer* ASME **92**: 595-609.

Bergles, A.E. and Rohsenow, W.M. 1964, "The Determination of Forced-Convection Surface-Boiling Heat Transfer," *Journal of Heat Transfer*, ASME **86**:365-372.

Bjorge, R. W., Hall, G. R., and Rohsenow, W. M., 1982, "Correlation of Forced Convection Boiling Heat Transfer Data," *International Journal of Heat and Mass Transfer* **25**:753–757.

Bowring, R. W., 1962, "Physical Model, Based on Bubble Detachment and Calculation of Steam Voidage in the Subcooled Region of a Heated Channel," *Institute for Atom Energie Rep.* HRP-I.O, Oslo, Norway 3.

Chen, J. C., 1966, "A Correlation for Boiling Heat Transfer to Saturated Fluids In Convective Flow," *Industrial and Engineering Chemistry, Process Design and Development* **5**: 322-329.

Global Digital Central
ISSN: 2151-8629

Chul-Hwa Song, Nhan Hien Hoang, In-Cheol Chu, Dong-Jin Euh., 2017, "A bubble dynamics-based model for wall heat flux partitioning during nucleate flow boiling," *International Journal of Heat and Mass Transfer* **112**, 454–464. http://dx.doi.org/10.1016/j.ijheatmasstransfer.2017.04.128

Claudi Martin Callizo.,2010, "Flow boiling heat transfer in single channel vertical diameter of small diameter," Doctoral Thesis, Department of energy technology, Royal institute of technology, Stockholm, Sweden, 47-49.

Deam, J. R., and Mattox, R. N.,1970, "Interfacial Tension in Hydrocarbon Systems," *Journal of Chemical Engineering Data*, **15** (2): 216–222.

Flippov, L.P., 1968, "Research of liquid thermal conductivity at Moscow University," *International Journal of Heat Mass transfer:* **11**, 331-345.

Fu, B.R., Tsou, M.S., and Chin Pan., 2012,. "Boiling heat transfer and critical heat flux of ethanol–water mixtures flowing through a diverging microchannel with artificial cavities," *International Journal of Heat and Mass Transfer* **55**: 1807–1814. https://doi.org/10.1016/j.ijheatmasstransfer.2011.11.051

Gungor, K.E. and Winterton, R.H.S., 1986, "A general correlation for flow boiling in tubes and annuli," *International Journal of Heat Mass Transfer* **29**: 351-358.

Hanyang Gu, Shuo Chen, Da Liu, Yao Xiao., 2019," Experimental study on onset of nucleate boiling and flow boiling heat transfer in a 5X5 rod bundle at low flow rate," *International Journal of Heat and Mass Transfer* **137**: 727–739. https://doi.org/10.1016/j.ijheatmasstransfer.2019.03.156

Hyungdae Kim, Muritala Alade Amidu, Satbyoul Jung., 2018, "Direct experimental measurement for partitioning of wall heat flux during subcooled flow boiling: Effect of bubble areas of influence factor," *International Journal of Heat and Mass Transfer* **127:** 515–533. https://doi.org/10.1016/j.ijheatmasstransfer.2018.07.079

Kline, S. J., and McClintock, F. A., 1953, "Describing Uncertainties in Single-Sample Experiments," Mechanical Engineering 75: 3–8.

Liu, Z. and Winterton, R. H. S., 1991, "A General Correlation for Saturated and Subcooled Flow Boiling in Tubes and Annuli Based on a Nucleate Pool Boiling Equation," *International Journal of Heat Mass Transfer* **34**: 2759-2766.

Lixin Cheng and Dieter Mewes., 2006, "Review of two-phase flow and flow boiling of mixtures in small and mini channels," *International Journal of Multiphase Flow*: **32**, 183–207. https://doi.org/10.1016/j.ijmultiphaseflow.2005.10.001

Madhavi V Deshpande and Vivek V Ranade., 2013,"Two phase Boiling in small Channels: A Brief Review" Indian Academy of Science: **38** (6), 2083-1126.

Mcneil, D.A., Raeisi, A.H., Kew, P.A. and Bobbili, P.R., 2010, "A comparison of flow boiling heat transfer in in-line mini pin fin and plane channel flows," *Applied Thermal Engineering* **30**: 2412-2428. https://doi.org/10.1016/j.applthermaleng.2010.06.011

Minxia Li, Chaobin Dang and Eiji Hihara., 2012, "Flow boiling heat transfer of HFO1234yf and R32 refrigerant mixtures in a smooth horizontal tube: Part I. Experimental investigation," *International Journal of Heat and Mass Transfer* **55**: 3437–3446. https://doi.org/10.1016/j.ijheatmasstransfer.2012.03.002

Minxia, L., Chaobin, D., and Eiji, H., 2013, "Flow boiling heat transfer of HFO1234yf and R32 refrigerant mixtures in a smooth horizontal tube: Part II. Prediction method," Int. J. of Heat and Mass Transfer **64**: 91-608. 10.1016/j.ijheatmasstransfer.2013.04.047

Moles, F.D and Shaw, F.G., 1972, "Boiling heat transfer to subcooled liquids under condition of forced convection," *Trans Institute Chemical. Engineering*, **50**: 76–84.

Satish G. Kandlikar., 1998, "Boiling heat transfer with binary mixture: Part-I, A theoretical modeling for pool boiling," J. of Heat Transfer, ASME **120:** 380-387.

Suhas, B.G and Sathyabhama.A., 2017, "Bubble dynamics of water-ethanol mixture during subcooled flow boiling in a conventional channel," *Applied Thermal Engineering* **113:** 1596–1609. https://doi.org/10.1016/j.applthermaleng.2016.11.126

Suhas, B.G. and Sathyabhama, A., 2017, "Experimental Investigation of Heat Transfer Coefficient and Correlation Development for Subcooled Flow Boiling of Water–Ethanol Mixture in Conventional Channel," *Journal of Thermal Science and Engineering application*, ASME **9**(4):041003-11. https://doi.org/10.1115/1.4036202

Suhas B.G and Sathyabhama.A., 2018, "Heat transfer and force balance approaches in bubble dynamic study during subcooled flow boiling of water–ethanol mixture," *Experimental Heat Transfer*, Taylor and Francis **31**(1): 1-21. https://doi.org/10.1080/08916152.2017.1328469

Suhas B.G and Sathyabhama.A., 2018, Experimental study on forced convective and subcooled flow boiling heat transfer coefficient of water-ethanol mixtures: An application in cooling of heat dissipative devices, *Heat and Mass Transfer*, Springer **54**: 277-290. 10.1007/s00231-017-2122-4

Sekoguchi, K., Tanaka, O., Esaki, S., and Imasaka, T., 1980, "Prediction of void fraction in subcooled and low quality boiling regions," *Bulletin of the JSME* **23**:1475-1482.

Unal, H. C., 1975, "Determination of the initial point of net vapor generation in flow boiling systems," *International Journal of Heat and Mass Transfer* **18:**1095-1099.

Vijay, K.D and Gopinath.W., 2006, "Heat Transfer and Wall Heat Flux Partitioning During Subcooled Flow Nucleate Boiling—A Review" *Journal of Heat Transfer*, ASME **128:**1242-1256. https://doi.org/10.1115/1.2349510

Vijay K.D, Hari, Abharjith and Ding, L., 2007, "Bubble Dynamics and Heat Transfer during Pool and Flow Boiling," *Heat Transfer Engineering*, Taylor and Francis, **28**: 608–624 https://doi.org/10.1080/01457630701266421

Weiwei, C. and Fang, X., 2014, "A Note on the Chen Correlation of Saturated Flow Boiling Heat Transfer," *Journal of Refrigeration* **48**:100–104.